Guanine base stacking in G-quadruplex nucleic acids

Christopher Jacques Lech, Brahim Heddi, and Anh Tuân Phan*

Division of Physics and Applied Physics
School of Physical and Mathematical Sciences,
Nanyang Technological University, Singapore 637371

Supplementary Data

*Corresponding author: phantuan@ntu.edu.sg

SUPPLEMENTARY DATA CONTENTS

Table. S1. Partial atomic charges used in MM Energy landscapes

Atom Name	Charge
N9	-0.3944
H9[a]	0.3609
C8	0.1466
H8	0.1619
N7	-0.5593
C5	0.2643
C6	0.4084
O6	-0.5245
N1	-0.3996
H1	0.3239
C2	0.6177
N2	-0.9282
H21	0.4288
H22	0.4288
N3	-0.5981
C4	0.2628

[a] H9 represents the hydrogen atom attatched to the N9 atom linking the guanine base to the sugar backbone in DNA.

Table. S2. Summary and statistics of crystallographic structures cataloged

PDB	Sequence	Description	Res. *(Å)*	Statistics of Rotation *(deg)* / Separation *(Å)*						Ref.
				Core Stacking			Interface Stacking			
				Type	N	Mean(σ)	Type	N	Mean(σ)	
1KF1	$d[AG_3(T_2AG_3)_3]$	*Telomeric* DNA Intramolecular Parallel Propeller Quadruplex – K^+	2.10	A/A	8	61.7(0.9) 3.42(0.08)	5'-5' 5/6-ring	2	56.2(1.9) 3.38(0.05)	(20)
1K8P	$d[^{Br}UAG_3{}^{Br}UTAG_3T]_2$	*Telomeric* DNA Bimolecular Parallel Propeller Quadruplex – K^+	2.40	A/A	8	60.2(3.6) 3.32(0.06)	-	-	-	(20)
2HRI	$d[TAG_3T_2AG_3]_2$	*Telomeric* DNA Bimolecular Parallel Propeller Quadruplex – K^+ + porphyrin TMPyP4	2.09	A/A	8	63.4(2.7) 3.36(0.05)	3'-3' 6-ring	2	46.0(0.9) 3.43(0.01)	(26)
3CCO	$d[TAG_3T_2AG_3T]_2$	*Telomeric* DNA Bimolecular Parallel Propeller Quadruplex – K^+ + tetra-substituted naphthalene diimide	2.20	A/A	4	63.0(10.1) 3.42(0.15)	5'-5' 5-ring	1	86.5(-) 3.46(-)	(27)
3CDM	$d[TA(G_3T_2A)_3G_3]$	*Telomeric* DNA Intramolecular Parallel Propeller Quadruplex – K^+ + tetra-substituted naphthalene diimide	2.10	A/A	16	62.3(2.3) 3.36(0.06)	-	-	-	(27)
3CE5	$d[TAG_3T_2AG_3T]_2$	*Telomeric* DNA Bimolecular Parallel Propeller Quadruplex – K^+ + BRACO-19	2.50	A/A	8	63.1(1.2) 3.46(0.11)	-	-	-	(57)
3QCR	$d[TAG_3T_2AG_3]_2$	*Telomeric* DNA Bimolecular Parallel Propeller Quadruplex – K^+ + acridine ligand	3.2	A/A	4	60.6(0.7) 3.20(0.12)	-	-	-	(58)
3IBK	$r[^{5Br}UAG_3U_2AG_3U]_2$	*Telomeric* RNA Bimolecular Parallel Propeller Quadruplex – K^+	2.20	A/A	8	60.9(4.9) 3.40(0.08)	-	-	-	(36)
3MIJ	$r[UAG_3U_2AG_3U]_2$	*Telomeric* RNA Bimolecular Parallel Propeller Quadruplex – K^+ + acridine ligand	2.60	A/A	4	63.6(4.1) 3.40(0.11)	-	-	-	(58)
2AVH	$d[G_4T_3G_4]_2$	DNA Bimolecular (2+2 ↑•↓•↑•↓) Edgewise quadruplex – K^+	1.50	S/A A/S	4 2	81.8(1.6) 3.47(0.07) 30.4(2.1) 3.66(0.05)	-	-	-	(23)
2AVJ	$d[G_4{}^{Br}UT_2G_4]_2$	DNA Bimolecular (2+2 ↑•↓•↑•↓) and (2+2 ↑•↑•↓•↓) Edgewise quadruplex – K^+	2.39	S/A A/S	24 12	83.2(2.5) 3.46(0.09) 29.0(1.5) 3.51(0.08)	Mixed 5'-3' Partial 6-ring	4	26.2(1.5) 3.50(0.08)	(23)
1JPQ	$d[G_4{}^{Br}UT_3G_4]_2$	*Oxytricha* DNA Bimolecular (2+2 ↑•↑•↓•↓) Diagonal quadruplex – K^+	1.60	S/A A/S	8 4	83.0(2.0) 3.48(0.12) 29.5(1.3) 3.50(0.05)	-	-	-	(65)

1JRN	$d[G_4T_4G_4]_2$	*Oxytricha* DNA Bimolecular (2+2 ↑•↑•↓•↓) Diagonal quadruplex – K^+	2.00	S/A A/S	16 8	82.7(2.9) 3.47(0.14) 29.1(0.9) 3.53(0.08)	-	-	-	(65)
2HBN	$d[G_4T_4G_4]_2$	*Oxytricha* DNA Bimolecular (2+2 ↑•↑•↓•↓) Diagonal quadruplex – Tl^+	1.55	S/A A/S	16 8	82.8 (2.7) 3.49(0.12) 29.2(1.9) 3.57(0.04)	-	-	-	(67)
2GWQ	$d[G_4T_4G_4]_2$	*Oxytricha* DNA Bimolecular (2+2 ↑•↑•↓•↓) Diagonal quadruplex – K^+	2.00	S/A A/S	32 16	83.1(1.0) 3.46(0.10) 29.5(1.6) 3.54(0.07)	-	-	-	[a]
2GWE	$d[G_4T_4G_4]_2$	*Oxytricha* DNA Bimolecular (2+2 ↑•↑•↓•↓) Diagonal quadruplex – K^+	2.20	S/A A/S	48 24	83.0(2.8) 3.44(0.13) 29.3(1.6) 3.55(0.08)	-	-	-	[a]
1L1H	$d[G_4T_4G_4]_2$	*Oxytricha* DNA Bimolecular (2+2 ↑•↑•↓•↓) Diagonal quadruplex – K^+ + acridine ligand	1.75	S/A A/S	8 4	83.1(2.1) 3.42(0.10) 28.8(1.1) 3.56(0.07)	-	-	-	(66)
3EM2	$d[G_4T_4G_4]_2$	*Oxytricha* DNA Bimolecular (2+2 ↑•↑•↓•↓) Diagonal quadruplex – K^+ + acridine ligand	2.30	S/A A/S	8 4	84.0(3.0) 3.42(0.09) 28.7(1.6) 3.57(0.05)	-	-	-	(68)
3EQW	$d[G_4T_4G_4]_2$	*Oxytricha* DNA Bimolecular (2+2 ↑•↑•↓•↓) Diagonal quadruplex – K^+ + acridine ligand	2.20	S/A A/S	8 4	83.9(2.6) 3.43(0.08) 28.6(1.2) 3.53(0.06)	-	-	-	(68)
3ERU	$d[G_4T_4G_4]_2$	*Oxytricha* DNA Bimolecular (2+2 ↑•↑•↓•↓) Diagonal quadruplex – K^+ + acridine ligand	2.00	S/A A/S	8 4	83.8(2.5) 3.43(0.08) 28.9(0.9) 3.55(0.08)	-	-	-	(68)
3ES0	$d[G_4T_4G_4]_2$	*Oxytricha* DNA Bimolecular (2+2 ↑•↑•↓•↓) Diagonal quadruplex – K^+ + acridine ligand	2.20	S/A A/S	8 4	83.8(1.5) 3.46(0.06) 29.0(1.0) 3.56(0.04)	-	-	-	(68)
3ET8	$d[G_4T_4G_4]_2$	*Oxytricha* DNA Bimolecular (2+2 ↑•↑•↓•↓) Diagonal quadruplex – K^+ + acridine ligand	2.45	S/A A/S	8 4	82.7(2.4) 3.52(0.09) 29.9(1.6) 3.59(0.08)	-	-	-	(68)

3EUI	$d[G_4T_4G_4]_2$	*Oxytricha* DNA Bimolecular (2+2 ↑•↑•↓•↓) Diagonal quadruplex – K^+ + acridine ligand	2.20	S/A A/S	16 8	84.2(1.9) 3.47(0.10) 30.3(0.7) 3.55(0.08)	-	-	-	(68)
3EUM	$d[G_4T_4G_4]_2$	*Oxytricha* DNA Bimolecular (2+2 ↑•↑•↓•↓) Diagonal quadruplex – K^+ + acridine ligand	1.78	S/A A/S	8 4	83.5(1.9) 3.45(0.08) 29.0(0.8) 3.49(0.04)	-	-	-	(68)
3NYP	$d[G_4T_4G_4]_2$	*Oxytricha* DNA Bimolecular (2+2 ↑•↑•↓•↓) Diagonal quadruplex – K^+ + acridine ligand	1.18	S/A A/S	8 4	84.6(2.3) 3.60(0.07) 28.1(1.1) 3.71(0.04)	-	-	-	(69)
3NZ7	$d[G_4T_4G_4]_2$	*Oxytricha* DNA Bimolecular (2+2 ↑•↑•↓•↓) Diagonal quadruplex – K^+ + acridine ligand	1.10	S/A A/S	8 4	83.8(2.0) 3.44(0.07) 29.0(0.9) 3.56(0.03)	-	-	-	(69)
2GW0	$d[TG_4T]_4$	Tetramolecular parallel DNA quadruplex –Na^+/ Ca^{+2}	1.55	A/A	24	60.6(3.0) 3.35(0.06)	5'-5' 5-ring	4	81.5(0.7) 3.49 (0.04)	(24)
244D	$d[TG_4T]_4$	Tetramolecular parallel DNA quadruplex – Na^+	1.20	A/A	48	60.6(2.8) 3.41(0.05)	5'-5' 5-ring	8	83.0(0.4) 3.50 (0.02)	(17)
352D	$d[TG_4T]_4$	Tetramolecular parallel DNA quadruplex – Na^+	0.95	A/A	48	60.9(3.1) 3.34(0.05)	5'-5' 5-ring	8	82.7(0.5) 3.42(0.03)	(18)
1O0K	$d[TG_4T]_4$	Tetramolecular parallel DNA quadruplex – Na^+ + daunomycin ligand	1.17	A/A	12	59.1(4.2) 3.27(0.04)	-	-	-	(59)
1S45	$d[TG_4T]_4$	Tetramolecular parallel DNA quadruplex – Na^+/Tl^+	2.20	A/A	24	61.8(2.6) 3.42(0.09)	5'-5' 5-ring	4	84.5(0.7) 3.59(0.02)	(21)
1S47	$d[TG_4T]_4$	Tetramolecular parallel DNA quadruplex – Na^+/Tl^+	2.50	A/A	36	62.5(3.3) 3.45(0.16)	5'-5' 5-ring	4	85.1(1.8) 3.60(0.07)	(21)
1V3P	$d[G^{5I}CGAGAGC]_4$	Octamolecular DNA quadruplex – K^+	2.30	-	-	-	5'-5' 5/6-ring	1	57.1(-) 3.47(-)	(22)
1P79	$[r(UGUG_2U)]_4$	Tetramolecular parallel Bulged RNA quadruplex – K^+	1.10	S/A A/A	1 1	77.7(-) 3.40(-) 61.9(-) 3.41(-)	-	-	-	(60)
2AWE	$r[U^{8Br}GGUGU]_4$	Tetramolecular parallel Bulged RNA quadruplex – K^+	2.10	S/A A/A B [b]	8 8	82.2(0.8) 3.57(0.04) 35.7(0.9) 3.53(0.06)	-	-	-	(70)

2GRB	r[^{5Br}UGIGGU]$_4$	Tetramolecular parallel RNA quadruplex – K^+	1.40	A/A	8	65.5(0.9) 3.52(0.04)	-	-	-	(63)
1J6S	[r(^{Br}UGAG$_2$U)]$_4$	Tetramolecular parallel RNA quadruplex –Ba^{2+}	1.40	A/A	4	65.7(0.5) 3.46(0.05)	-	-	-	(61)
1J8G	r[UG$_4$U]$_4$	Tetramolecular parallel RNA quadruplex – Sr^{2+}	0.61	A/A	12	60.6(3.9) 3.31(0.04)	5'-5' 6-ring	2	37.2(0.7) 3.39(0.00)	(19)
1MDG	[r(U)d(^{Br}G)r(AG$_2$U)]$_4$	Tetramolecular parallel RNA quadruplex - Na^+	1.50	A/A	1	64.5(-) 3.39(-)	-	-	-	(62)
2O4F	d[TG$_4$T]$_4$	Tetramolecular parallel DNA quadruplex – Na^+	1.50	A/A	24	61.2(2.6) 3.42(0.06)	5'-5' 5-ring	4	82.7(0.2) 3.63(0.03)	(25)

G-quadrupex structures included in this work were obtained by searching the Protein Data Bank using the following keywords: quadruplex(es); tetrad(s); tetraplex(es); G4. PDB Entries 1D59 and 1JB7 were not examined in this work. Statistics presented are for experimental stacked guanines pairs from a single PDB compared to model stacked guanine pairs.

[a] PDB Entries from work not yet published.

[b] *Anti/Anti* Stacking present with a one residue bulge.

Table. S3. Sub-classification of stacked guanines within the G-tetrad core of cataloged crystallographic G-quadruplex structures

Classification	Count	Rotation (Deg)		Seperation (Å)		Associated Tetrad Energy [a] (kcal/mol)
		Mean	s.d	Mean	s.d	
Telomeric – Anti → Anti	68	62.07	3.57	3.376	0.100	**5.73**
- *DNA*	56	62.13	3.35	3.370	0.100	**5.70**
- *RNA*	12	61.78	4.62	3.402	0.088	**5.87**
- *Drug*	44	62.70	3.51	3.373	0.107	**5.77**
- *No Drug*	24	60.91	3.44	3.380	0.082	**5.65**
- *Intramolecular*	24	62.11	1.97	3.381	0.070	**5.76**
- *Bimolecular*	44	62.04	4.21	3.3773	0.111	**5.71**
Oxythricha – Syn → Anti	236	83.25	2.41	3.462	0.109	**8.55**
- *Drug*	88	83.78	2.18	3.465	0.096	**8.62**
- *No Drug*	148	82.94	2.49	3.460	0.117	**8.51**
- *K^+ Salt*	220	83.29	2.39	3.460	0.108	**8.53**
- *Tl^+ Salt*	16	82.76	2.71	3.491	0.125	**8.84**
- *Diagonal Loop*	208	83.29	2.42	3.461	0.112	**8.55**
- *Edgewise Loop*	28	82.97	2.38	3.465	0.090	**8.56**
- *↑•↑•↓•↓ Strand Direction*	16	83.52	2.53	3.456	0.099	**8.51**
- *↑•↓•↑•↓ Strand Direction*	12	82.25	2.02	3.477	0.078	**8.40**
Oxythricha – Anti → Syn	118	29.23	1.40	3.549	0.076	**11.53**
- *Drug*	44	29.14	1.19	3.565	0.076	**11.90**
- *No Drug*	74	29.28	1.51	3.540	0.075	**11.31**
- *K^+ Salt*	110	29.23	1.37	3.548	0.078	**11.50**
- *Tl^+ Salt*	8	29.19	1.91	3.568	0.035	**11.95**
- *Diagonal Loop*	104	29.23	1.39	3.552	0.073	**11.59**
- *Edgewise Loop*	14	29.21	1.55	3.531	0.096	**11.13**
- *↑•↑•↓•↓ Strand Direction*	8	28.49	1.29	3.493	0.101	**10.61**
- *↑•↓•↑•↓ Strand Direction*	6	30.17	1.43	3.582	0.065	**9.98**
Tetramer – Anti → Anti	242	61.32	3.20	3.391	0.096	**5.75**
- *DNA*	216	61.11	3.09	3.390	0.095	**5.73**
- *RNA*	26	63.08	3.62	3.404	0.103	**5.99**
- *K^+ Salt*	9	65.09	1.47	3.507	0.055	**7.85**
- *Na^+ Salt*	165	60.99	3.13	3.381	0.082	**5.66**
- *Ca^{+2} Salt*	8	60.26	1.67	3.339	0.049	**5.34**
- *Tl^+ Salt*	44	61.76	3.07	3.432	0.129	**6.39**
- *Sr^{+2} Salt*	8	63.16	1.21	3.310	0.049	**5.52**
- *Ba^{+2} Salt*	4	65.69	0.53	3.459	0.049	**6.96**
- *No Salt*	4	55.45	0.41	3.306	0.017	**4.47**

[a] Associated Tetrad energy is interpolated from MP2/6-31G*(0.25) Landscapes based off average rotation and separation values for different sub-classes

Table. S4. Summary and statistics of NMR G-quadruplex structures cataloged

PDB	Sequence	Description	Res. *(Å)*	Statistics of Rotation *(deg)* / Seperation *(Å)*						Ref.
				Core Stacking			Interface Stacking			
				Type	N	Mean(σ)	Type	N	Mean(σ)	
139D	$d[T_2G_4T]_4$	DNA Intermolecular Parallel Quadruplex – K^+	-	A/A	12	60.1(5.0) 3.17(0.08)	-	-	-	(82)
143D	$d[AG_3(T_2AG_3)_3]$	DNA Intramolecular Telomeric (2+2 ↑•↓•↑•↓) Quadruplex – Na^+	-	S/A	4	79.0(5.3) 3.45(0.12)	-	-	-	(83)
				A/S	4	29.8(9.2) 3.74(0.10)				
148D	$d[G_2T_2G_2TGTG_2T_2G_2]_2$	DNA Intermolecular Thrombin aptamer (2+2 ↑•↓•↑•↓) Quadruplex – K+	-	S/A	4	86.4(3.8) 3.55(0.57)	-	-	-	(84)
156D	$d[G_4T_4G_4]_2$	*Oxytricha* Intermolecular DNA (2+2 ↑•↑•↓•↓) Quadruplex – K+	-	S/A	8	85.7(4.8) 3.38(0.37)	-	-	-	(85)
				A/S	4	31.7(8.4) 3.39(0.32)				
186D	$d[(T_2G_4)_4]$	*Oxytricha* Intarmolecular DNA (3+1) Quadruplex – Na+	-	S/A	4	84.8(2.0) 3.38(0.25)	-	-	-	(71)
				A/A	3	63.9(10.8) 3.51(0.28)				
				S/S	1	15.1(-) 3.28(-)				
1A8N	$d[G_3\ CT_4\ G_3C]_2$	*Human Chromosomal repeat* DNA (2+2 ↑•↑•↓•↓) Quadruplex – Na+	-	S/A	4	88.3(1.5) 3.46(0.02)	-	-	-	(86)
1A8W	$d[G_3\ CT_4\ G_3C]_2$	DNA (2+2 ↑•↑•↓•↓) Quadruplex – K+	-	S/A	4	81.6(0.5) 3.61(0.03)	-	-	-	(87)
1AFF	$d[T_2AG_3]_4$	Tetrameric DNA Quadruplex –	-	S/A	4	84.0(10.1) 3.76(0.04)	-	-	-	(88)
2GKU	$d[T_2(G_3T_2A)_3\ G_3A]$	Telomeric DNA (3+1) Quadruplex – K+	-	A/A	3	61.1(6.4) 3.38(0.09)	-	-	-	(72)
				S/S	1	30.1(-) 3.55(-)				
				S/A	4	82.3(3.0) 3.57(0.18)				
2KZD	$d[AG_3IAG_4CTG_3AG_3C]$	DNA (3+1) Quadruplex – K+	-	A/A	3	59.9(3.1) 3.33(0.14)	-	-	-	(74)
				S/S	1	28.2(-) 3.93(-)				
				S/A	4	85.8(2.1) 3.93(0.15)				

				A/A	2	64.4(1.74) 3.37(0.12)					
2KAZ	d[$G_3ACGTAGTG_3$]$_2$	DNA (2+2 ↑•↑•↓•↓) Diagonal Quadruplex – K+	-	S/S	2	27.9(2.2) 3.53(0.21)	-	-	-	(73)
				S/A	4	85.9(2.6) 3.42(0.08)					
1MYQ	d[$(GGA)_4$]	DNA Parallel Propeller Quadruplex – K+	-	-	-	-	5'-5' 5/6-ring	4	60.1(7.5) 3.26(0.23)	(28)
1MY9	r[$G_2AG_2U_4G_2AG_2$]	RNA Parallel Propeller Quadruplex – K+	-	-	-	-	5'-5' 5-ring 5/6-ring	3 1	84.2(2.4) 3.00(0.19) 71.3(-) 3.93(-)	(30)
1EEG	d[$(GGA)_2$]$_2$	DNA Biomolecular Parallel Propeller Quadruplex – Na+	N/A	-	-	-	5' ↔ 5' ND	-	-	(89)
1OZ8	d[$(GGA)_8$]	DNA Linked Dimeric Parallel Propeller Quadruplex – Na+/K+	-	-	-	-	Linked 5' ↔ 5' 5/6-ring	4	61.7(5.0) 3.57(0.50)	(31)
1JJP	d[$G_3AG_2T_3G_3AT$]$_2$	DNA Interlocked Dimeric Quadruplex – Na+	-	-	-	-	Locked 5-ring	-	-	(29)
2RQJ	r[$(GGA)_4$]	RNA Parallel Propeller Quadruplex – K+	-	-	-	-	5'-5' 5-ring 5/6-ring	2 2	77.2(0.1) 3.26(0.11) 68.5(0.2) 3.32(0.06)	(33)
1Y8D	d[$G_4TG_3AG_2AG_3T$]$_2$	DNA Interlocked Dimeric Quadruplex – K+	-	-	-	-	Locked 5-ring	-	-	(32)
2LE6	d[GIGT(G_3T)$_3$]	DNA Parallel Propeller Quadruplex – K+	-	-	-	-	5'-5' 5/6-ring	4	56.8(1.94) 3.37(0.04)	(34)
2WCN	d[G(^{LNA}G)G(^{LNA}G)T_4G(^{LNA}G)G(^{LNA}G)]	DNA V4 folded Quadruplex – K+	-	-	-	-	Locked P 6-ring	-	-	(75)

G-quadrupex structures included in this work cover a range of different folding topologies and include structures in which stacked guanine tetrads are presented at the interface between monomer G-quadruplexes. Statistics presented are for experimental stacked guanines pairs from a single PDB compared to model stacked guanine pairs.

Table S5: ΔE d_{tet}-profile (θ_{tet} = 60° same polarity) computed using various ion models (kcal/mol)

Ion Model	Distance						
	3	**3.1**	**3.2**	**3.3**	**3.4**	**3.5**	**3.6**
K+	-142.3	-149.5	-153.1	-154.2	-153.6	-151.8	-149.3
Na+	-164.0	-169.0	-170.6	-169.8	-167.5	-164.1	-160.2
2 Na+ [a]	9.2	2.2	-1.4	-2.6	-2.2	-0.8	1.1
None [b]	-15.6	-22.0	-25.2	-26.2	-25.7	-24.4	-22.5

[a] For the 2 Na+ model, an Na+ ion is located in the center of each tetrad. A total of 2 molecular fragments are considered for ΔE calculations, each fragment consisting of a G-tetrad with the in-plane Na+ ion.
[b] For None ion model, a total of 2 molecular fragments are considered for ΔE calculations, each fragment consisting of a G-tetrad.

Table S6: ΔE θ_{tet}-profile (d_{tet} = 3.4Å) same polarity computed using various ion models (kcal/mol)

Ion Model	Distance									
	0	**5**	**10**	**15**	**20**	**25**	**30**	**35**	**40**	**45**
K+	-142.7	-146.0	-151.8	-154.2	-153.7	-153.2	-153.6	-154.1	-154.5	-154.8
Na+	-156.3	-159.6	-165.5	-168.0	-167.5	-167.1	-167.5	-168.0	-168.5	-168.7
2 Na+ [a]	8.9	5.7	-0.1	-2.6	-2.2	-1.8	-2.2	-2.8	-3.4	-3.7
None [b]	-15.5	-18.8	-24.5	-26.7	-26.0	-25.5	-25.7	-26.0	-26.4	-26.5
	50	**55**	**60**	**65**	**70**	**75**	**80**	**85**	**90**	
K+	-154.5	-154.1	-153.6	-153.2	-153.7	-154.2	-151.8	-146.0	-142.7	
Na+	-168.5	-168.0	-167.5	-167.1	-167.5	-167.9	-165.5	-159.6	-156.3	
2 Na+ [a]	-3.4	-2.8	-2.2	-1.8	-2.2	-2.6	-0.1	5.7	8.9	
None [b]	-26.4	-26.0	-25.7	-25.5	-26.0	-26.7	-24.5	-18.8	-15.5	

[a] For the 2 Na+ model, an Na+ ion is located in the center of each tetrad. A total of 2 molecular fragments are considered for ΔE calculations, each fragment consisting of a G-tetrad with the in-plane Na+ ion.
[b] For None ion model, a total of 2 molecular fragments are considered for ΔE calculations, each fragment consisting of a G-tetrad.

Table S7: ΔE θ_{tet}-profile (d_{tet} = 3.4Å) opposite polarity computed using various ion models (kcal/mol)

Ion Model	Distance									
	0	**5**	**10**	**15**	**20**	**25**	**30**	**35**	**40**	**45**
K+	-151.3	-150.6	-149.3	-148.5	-148.0	-148.4	-150.6	-153.2	-153.9	-153.7
Na+	-165.0	-164.3	-163.1	-162.3	-161.9	-162.3	-164.5	-167.1	-167.9	-167.7
2 Na+ [a]	0.3	0.9	2.2	3.0	3.3	2.7	0.7	-1.9	-2.6	-2.5
None [b]	-24.1	-23.4	-22.0	-21.0	-20.4	-20.6	-22.6	-25.3	-26.1	-25.8
	50	**55**	**60**	**65**	**70**	**75**	**80**	**85**	**90**	
K+	-155.3	-157.8	-158.1	-156.0	-153.9	-152.6	-151.7	-151.3	-151.3	
Na+	-169.2	-171.6	-171.8	-169.7	-167.5	-166.3	-165.3	-165.0	-165.0	
2 Na+ [a]	-4.1	-6.6	-6.7	-4.5	-2.2	-0.7	0.3	0.5	0.3	
None [b]	-27.4	-29.9	-30.2	-28.2	-26.4	-25.4	-24.5	-24.1	-24.1	

[a] For the 2 Na+ model, an Na+ ion is located in the center of each tetrad. A total of 2 molecular fragments are considered for ΔE calculations, each fragment consisting of a G-tetrad with the in-plane Na+ ion.
[b] For None ion model, a total of 2 molecular fragments are considered for ΔE calculations, each fragment consisting of a G-tetrad

Text S1:

Bulged RNA sequences are those in which two nucleotides within the core have stacked guanine bases that are separated from each other sequentially by another nucleotide whose base does not form the guanine tetrad core. One RNA G-quadruplex forming sequence U^{Br}GGUGU demonstrates a unique Anti/Anti stacking arrangement due to this bulge (70). In this structure there is a Partial-5/6ring stacking very similar to that observed in *Anti/Anti* steps, except the stacking occurs between guanine bases from neighboring strands.

Text S2:

A series of QM energy profiles were computed to compare the effect of ion type on coordinated stacked tetrads (Supplementary Figure 6). Models were run with a central K^+, a central Na^+, two Na^+ ions in the tetrad plane, and no ion present. The rotational energy profiles for all of these models are very similar (Figure S5.B-C). However, ion type does affect the separation energy profile. When K+ is substituted with Na+, the energy minima is lowered (Figure S5A). The use of two Na+ ions is more similar to the curve of K+, except slightly flattened. Interestingly, the use of two Na^+ ions, one in the center of each tetrad, leads to an energy profile that is almost identical to model with no coordinating ion. In the presented Na^+-containing crystal structures (17,18,21,24,25,59,62), ions are found in a range between the two extremes explored in these models with the 2 Na^+ motif being slightly more observed. With this in mind we include all structures in the statistics used to derive relative experimental base stacking energies (Table 2).

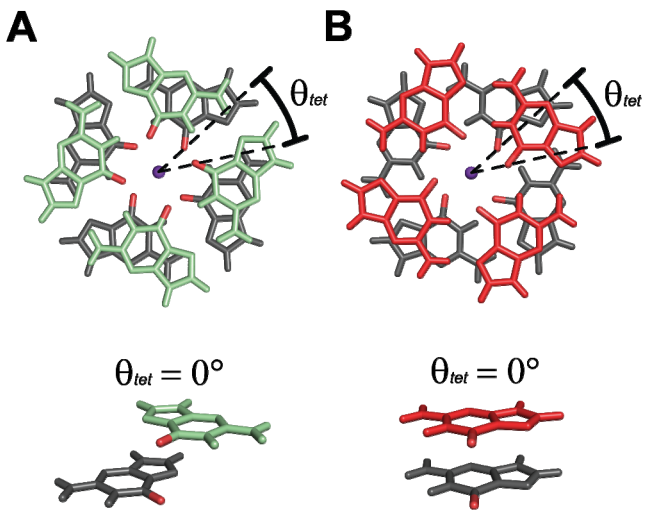

Figure S1: An illustration of the (θ_{tet}) measurement is shown for (A) opposite-polarity and (B) same-polarity stacked G-tetrad models. Relative rotation is arbitrarily defined to be 0° when the O6 atoms of stacked guanines are at their closest (bottom).

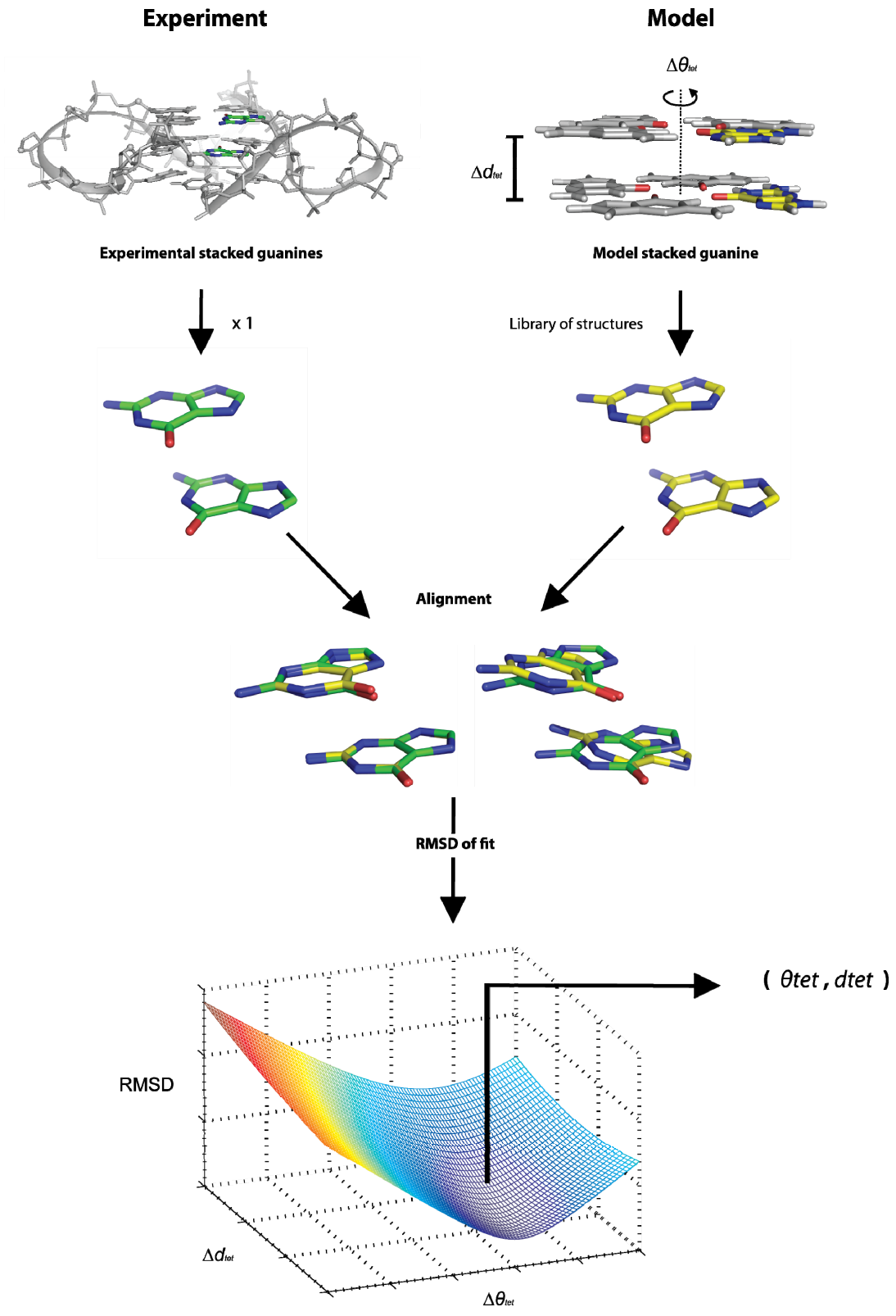

Figure S2: Experimental Characterization Procedure: Stacked guanine bases from experimental tetrads are fit to stacked guanines from a library of model stacked guanine tetrads. The relative rotation (θ_{tet}) and separation (d_{tet}) are determined by the model stacked guanine pair that provides the lowest RMSD fit to the experimental guanine pair.

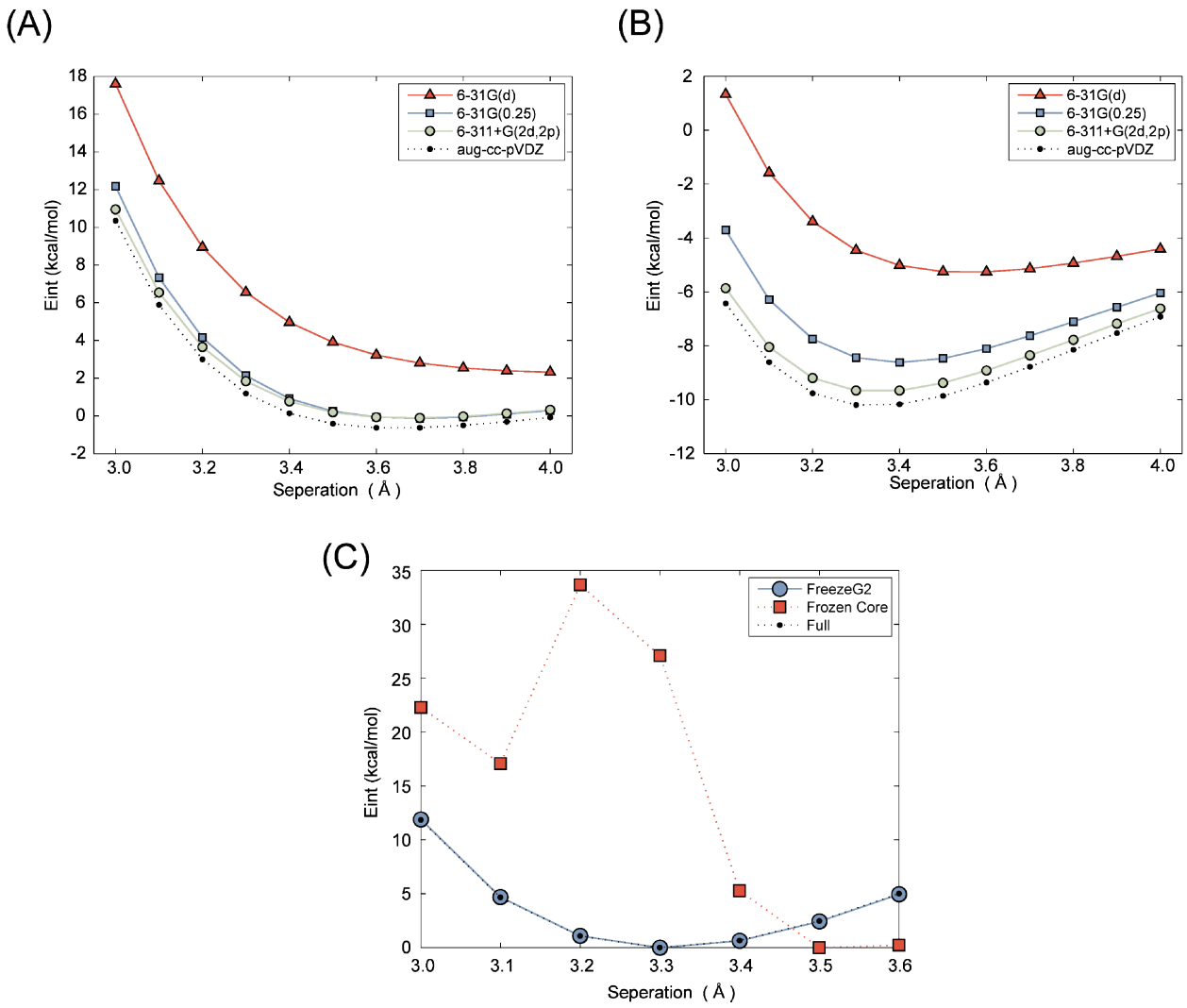

Figure S3: Effect of quantum chemical methods and basis set: **(A-B)** Separation energy profile of stacked parallel guanine dimers for **(A)** 0° rotation through center of mass and **(B)** 180° rotation through center of mass. **(C)** Effect of electron correlation on separation energy profiles: Profiles were carried out using Frozen Core (□), G2 convention (○), and all electron (•) correlation methods on K+-coordinated stacked guanine tetrads exhibiting same-polarity stacking with a relative rotation of 60°. The frozen core approximation is inadequate in modeling K+ coordination while the use of the G2 convention is almost identical to including all electrons in post Hartree-fock MP2 electron correlation calculations. Energy profiles in this graph have been individually normalized with their individual minima interaction energy taken to be zero.

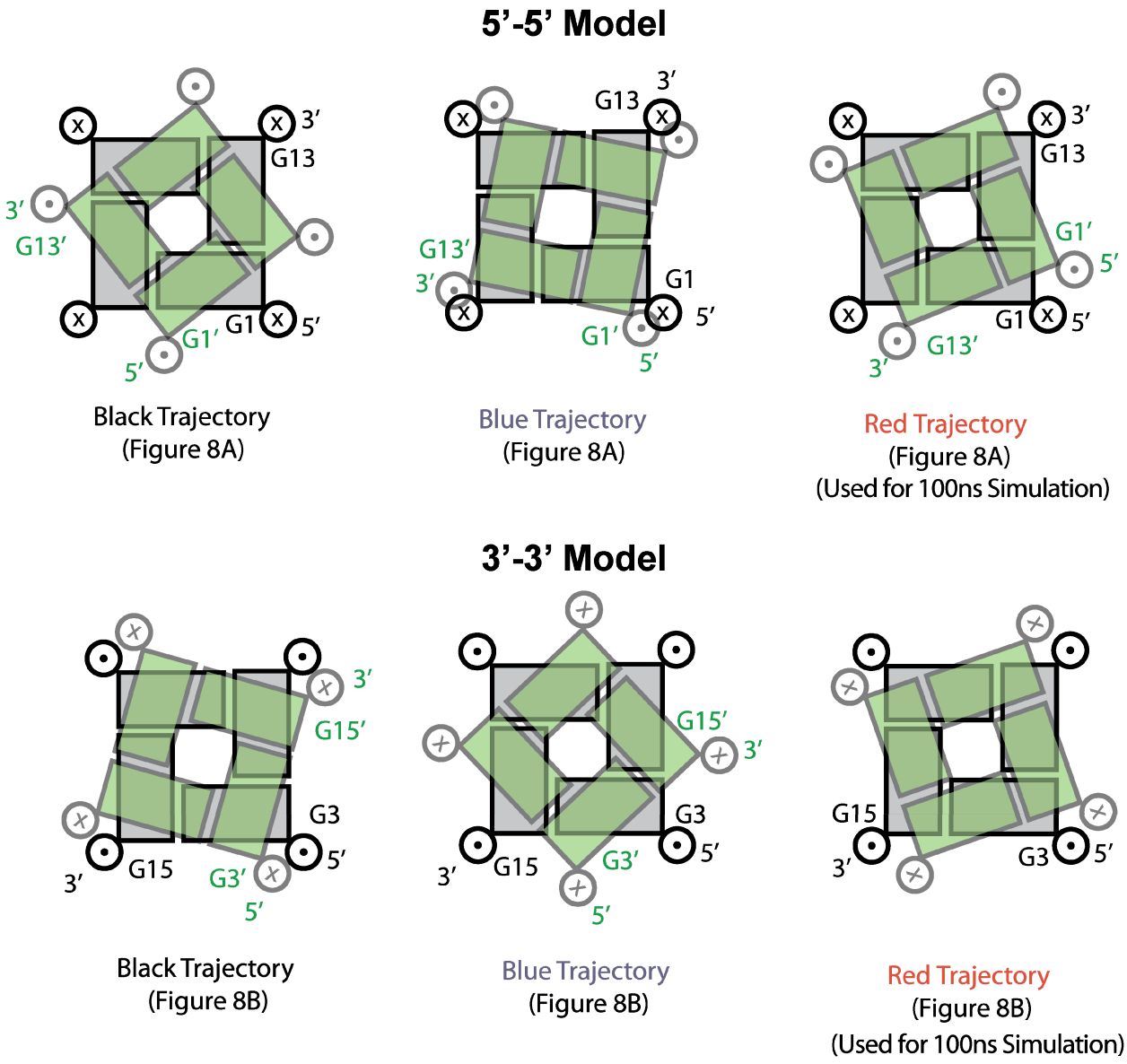

Figure S4: Schematic of Initial Stacking interface geometries for MD simulations: Diagrams depicting the orientation and approximate rotational geometries of interface tetrads in the 5'-5' and 3'-3' models stacked G-quadruplex formed by the sequence d[$(G_3T)_3G_3$] explored in this study. The interface stacking tetrads of the two G-quadrupex units are shown in grey and green. The 5'- and 3'-end strand of each G-quadruplex molecule are labeled as well as the 5'-end most and 3'-end most guanine participating in interface stacking. Relative strand directionality is indicated as (x) for going into the page and (•) as out of the page.

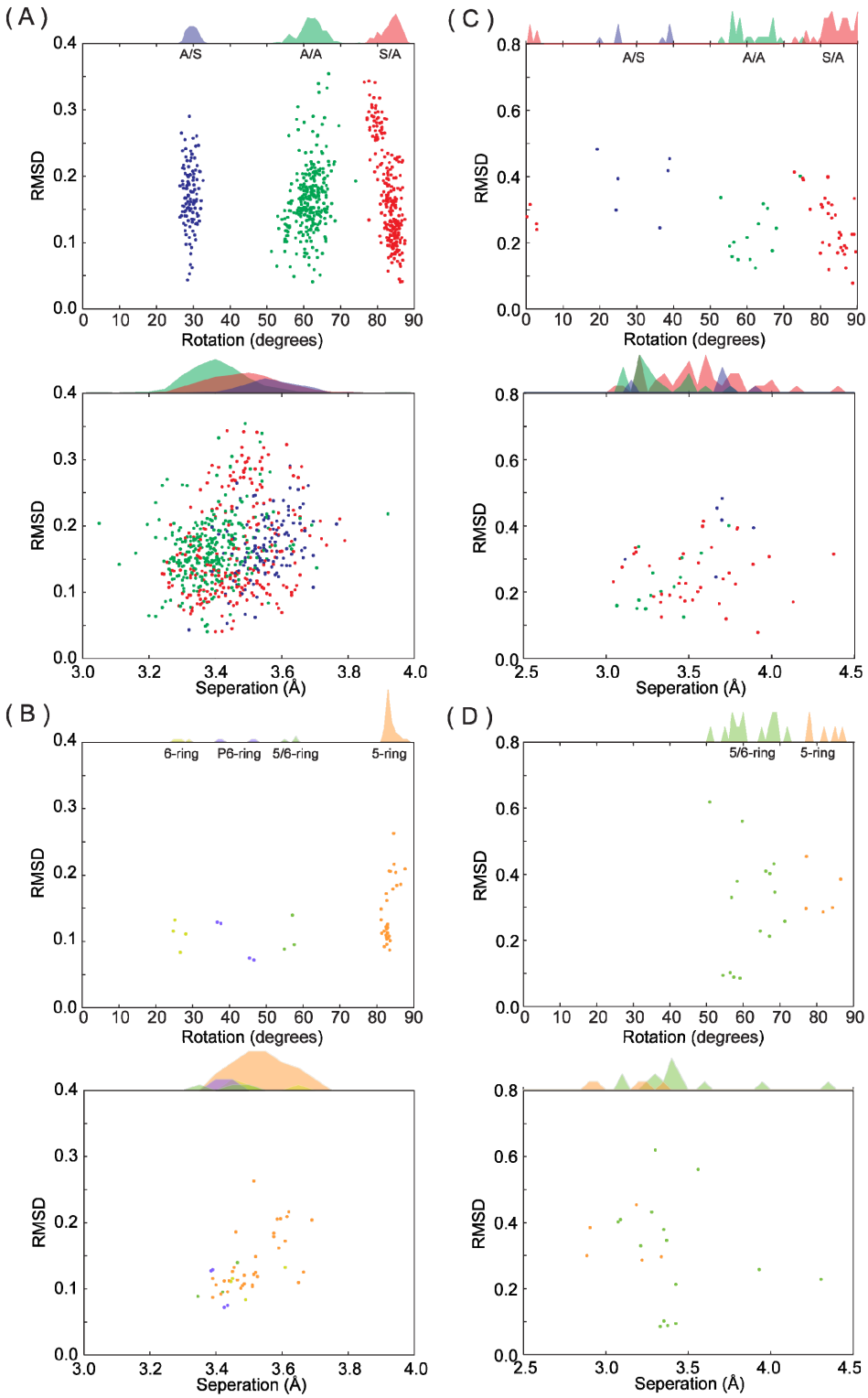

Figure S5: Plots of RMSD between experimental and model guanine pairs vs. relative rotation and tetrad separation: Data shown for (**A-B**) crystallographic structures and (**C-D**) NMR structures cataloged in this work. (**A and C)** Core stacking modes are shown with the following color codes: *Anti/Anti* (green); *Syn/Anti* (red); *Anti/Syn* (blue). (**B and D**) Interface stacking modes are shown with the following color codes: *Partial 6-ring* (yellow); *6-ring* (purple); *5/6-ring* (light green); *5-ring* (orange). Data represents the (C,N,O) atom RMSD between a pair of experimental stacked guanines and the best fitting model stacked guanine pair. (see Methods)

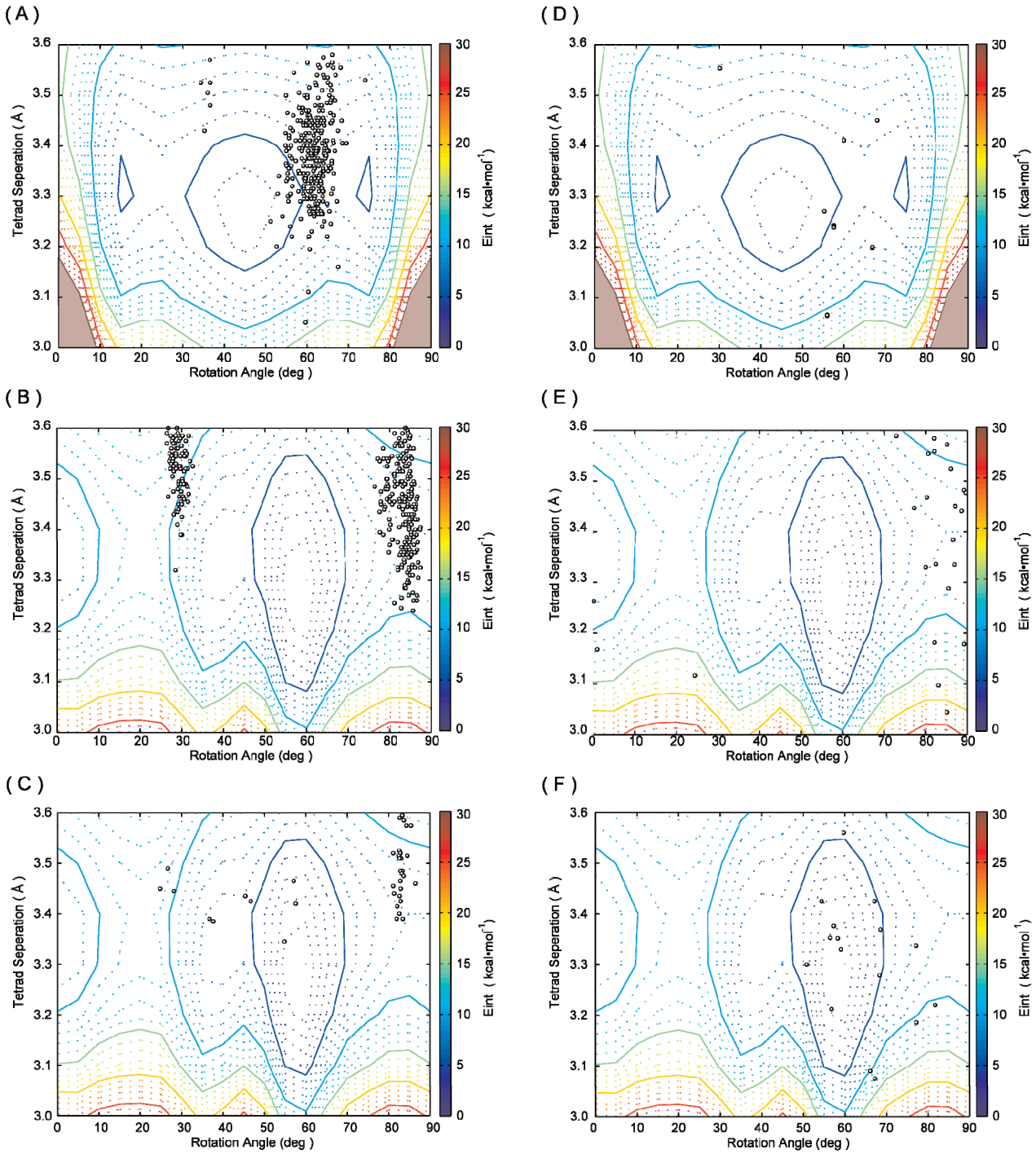

Figure S6: Raw data from cataloged structures super imposed on QM energy landscapes: **(A)** Crystallographic core guanines exhibiting same-polarity stacking. **(B)** Crystallographic core guanines exhibiting opposite-polarity stacking **(C)** Crystallographic interface guanines exhibiting opposite-polarity stacking. **(D)** NMR core guanines exhibiting same-polarity stacking. **(E)** NMR core guanines exhibiting opposite-polarity stacking **(F)** NMR interface guanines exhibiting opposite-polarity stacking.

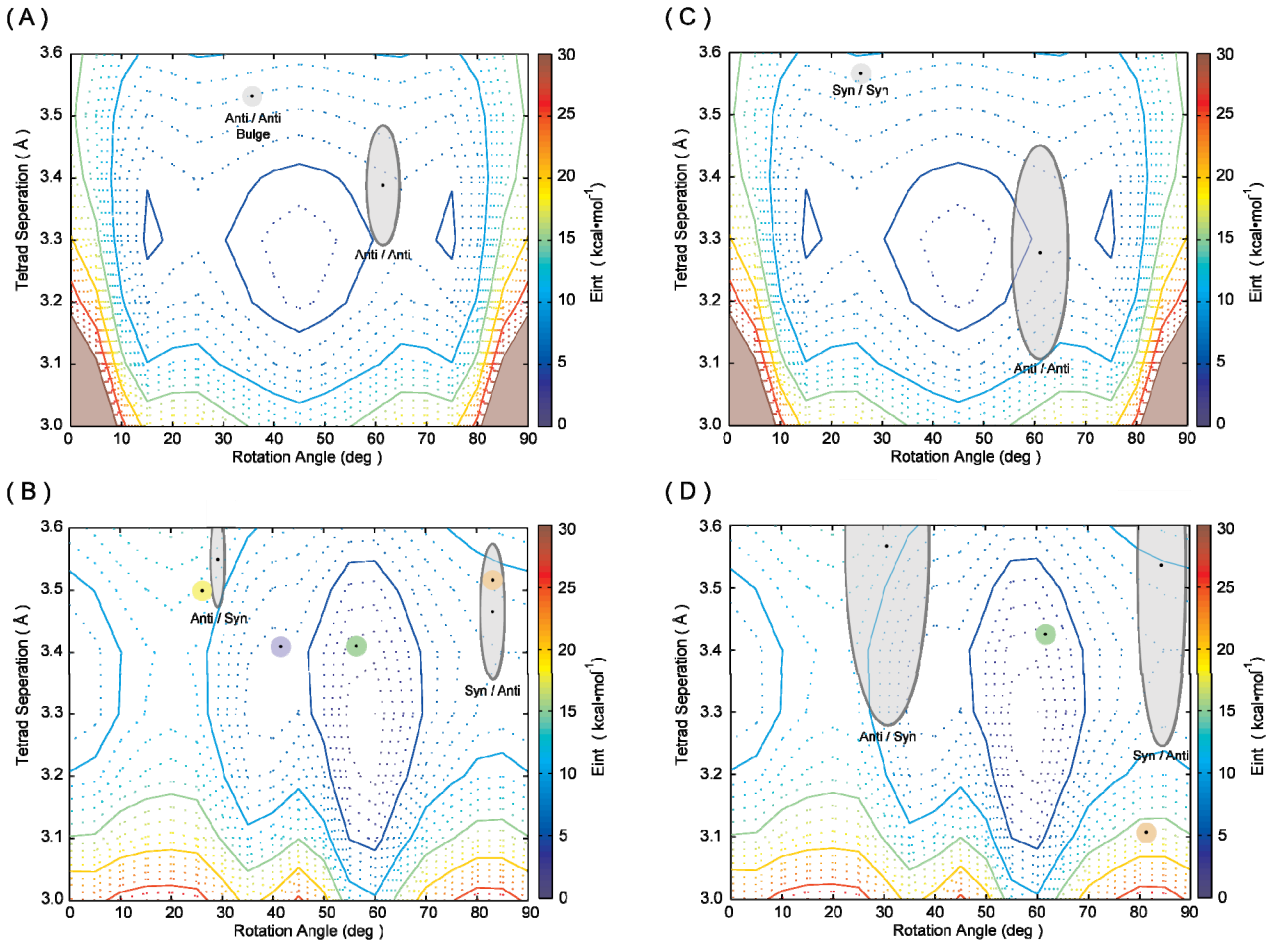

Figure S7: Statistical data from cataloged structures super imposed on QM energy landscapes: **(A)** Crystallographic guanines exhibiting same-polarity stacking. **(B)** Crystallographic guanines exhibiting opposite-polarity stacking. **(C)** NMR guanines exhibiting same-polarity stacking. **(D)** NMR guanines exhibiting opposite-polarity stacking Average core stacking modes (grey regions) and mean interface stacking modes (circles core coded as shown in Figure 5). Outlined regions have dimensions of the 1st standard deviation.

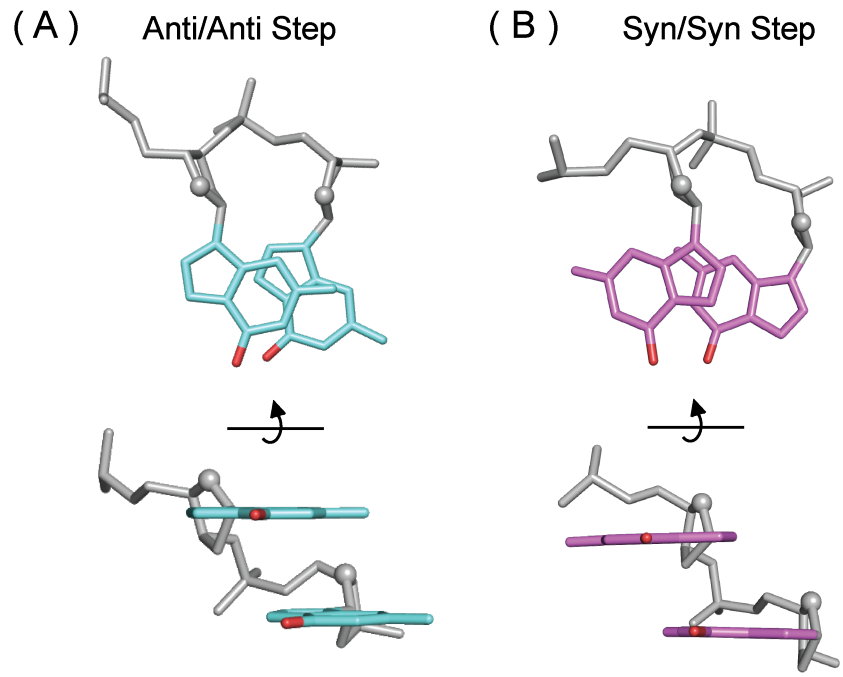

Figure S8: Illustrative comparison of **(A)** Anti/Anti stacking (PDB 1KF1) and **(B)** Syn/Syn stacking (PDB 2GKU). *Anti* and *Syn* guanines are shown in cyan and magenta respectively. O6 oxygen atoms are shown in red. O4' of the sugar is shown in spherical representation.

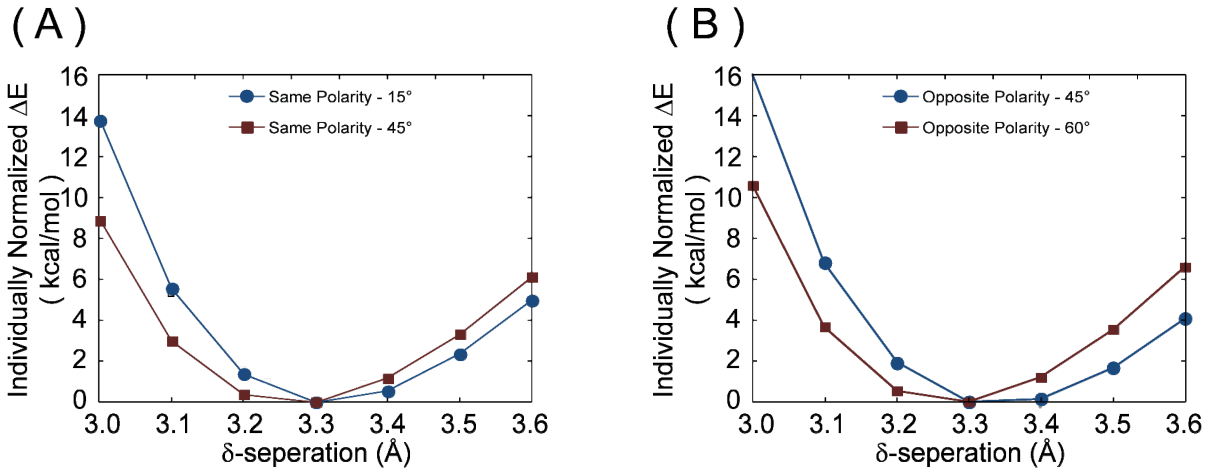

Figure S9: Stacking energy curves as a function of d_{tet} are shown for select θ_{tet} values for **(A)** same-polarity and **(B)** opposite-polarity stacked tetrads. Curves have been individually normalized to highlight minima.

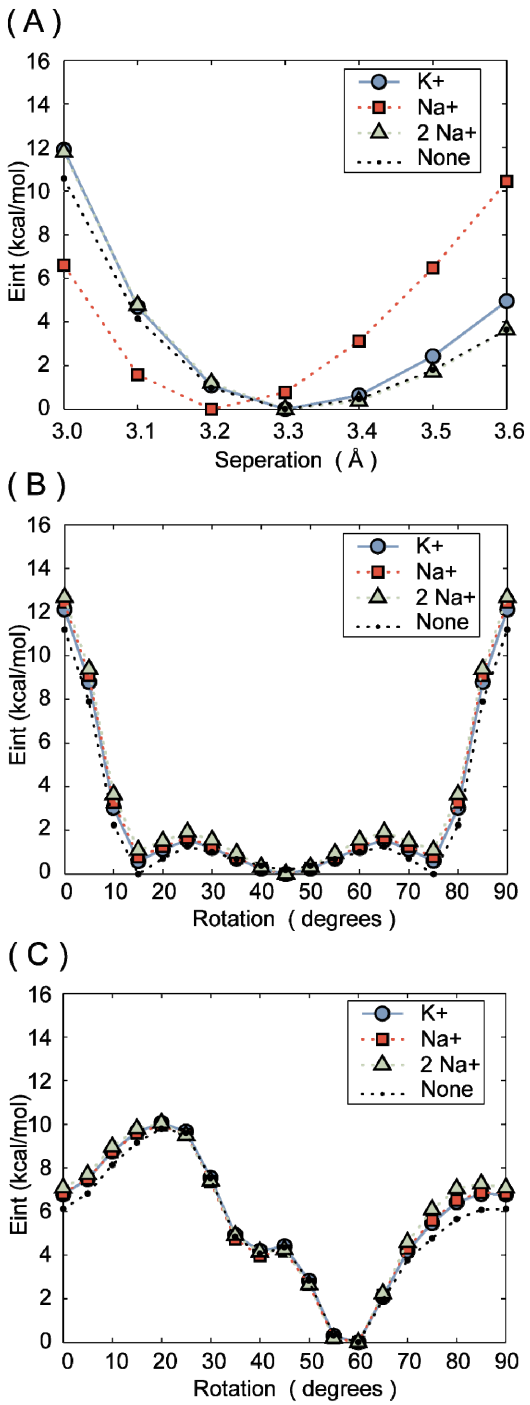

Figure S10: Effect of ion type on QM energy profiles of stacked G-tetrads containing central K^+ (○), central Na^+ (□), and two Na^+, one in the center of each tetrad (Δ): **(A)** Separation profile of 60° same-polarity stacked tetrads. Similar energy profiles are observed for the K^+ and two-Na^+ containing models. **(B)** Rotational energy profile of same-polarity stacked tetrads at 3.4 Å separation. **(C)** Rotational energy profile of opposite-polarity stacked tetrads at 3.4 Å separation. Energy profiles have been individually normalized with their individual minima Interaction energy taken to be zero.

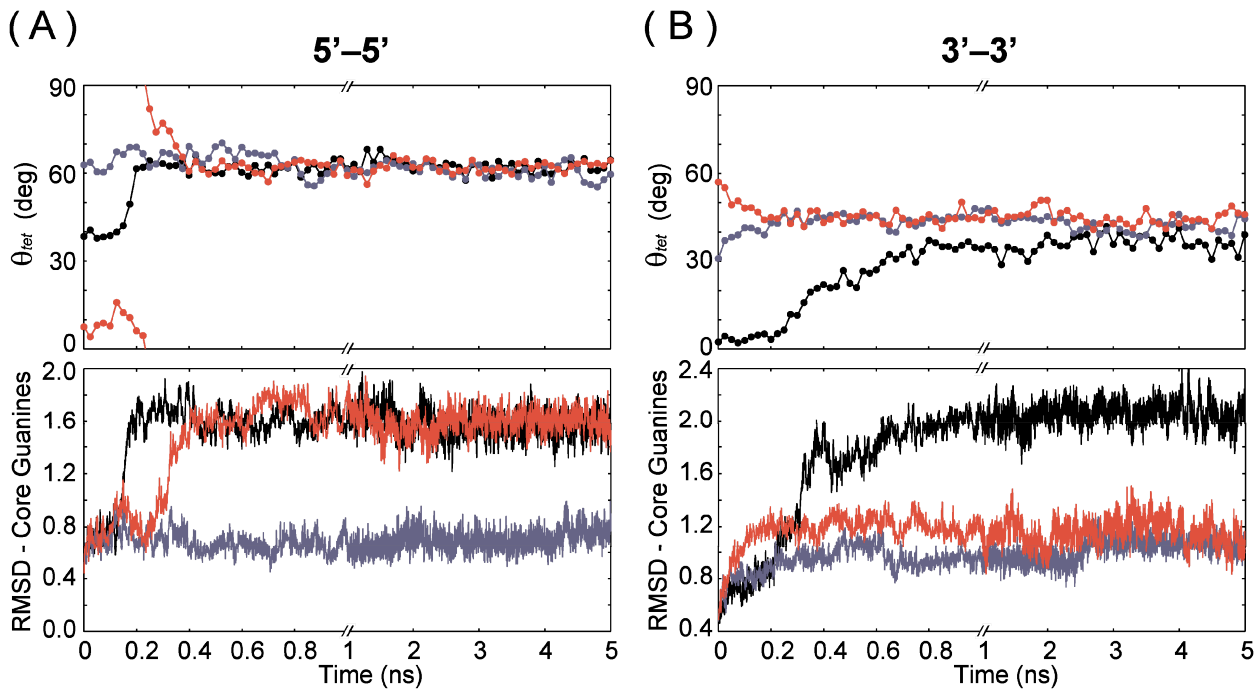

Figure S11: MD investigation of G-quadruplex G-tetrad stacking interfaces: 5 ns trajectories of stacked propeller G-quadruplexes formed by the sequences d[$(G_3T)_3G_3$] were run for (A) 5'–5' and (B) 3'–3' stacked G-quadruplexes. The average relative rotation (θ_{tet}) of interface guanines (top) and RMSD of core G-tetrad guanine bases (bottom) was characterized at regular intervals. Three different starting geometries of G-quadruplex stacking arrangements (Interface θ_{tet} varying by ~30°) are represented by black, blue, and red trajectories.

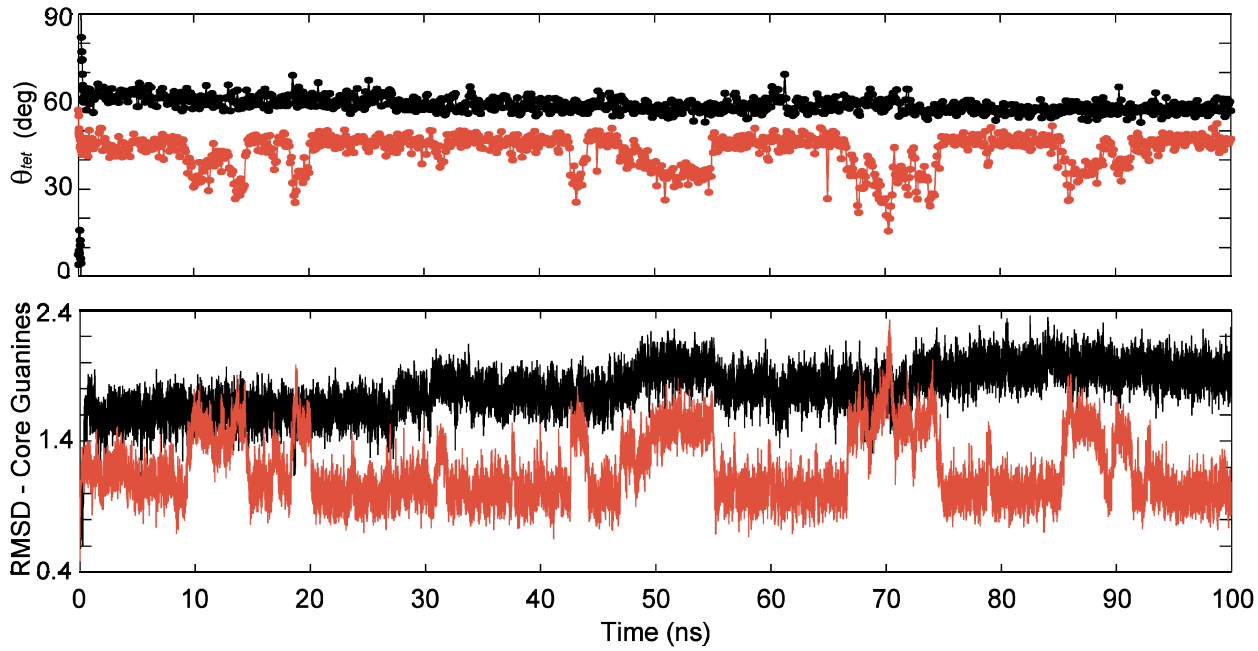

Figure S12: Extended MD simulations of 5'–5' and 3'–3' stacked G-quadruplexes: Long 100 ns trajectories were computed for a 5'–5' (black) and a 3'–3' (red) stacked G-quadruplex complex. Average relative rotation (θ_{tet}) of interface guanines (top) and RMSD of core G-tetrad guanine bases (bottom) was characterized at regular intervals.